CRYSTAL GROWTH & DESIGN

ARTICLE

pubs.acs.org/crystal

# Fast Precipitation of Acicular Goethite from Ferric Hydroxide Gel under Moderate Temperature (30 and 70 °C)

G. Montes-Hernandez,*[,†] P. Beck,[‡] F. Renard,[†,§] E. Quirico,[‡] B. Lanson,[†] R. Chiriac,[∥] and N. Findling[†]

[†]CNRS and University Joseph Fourier-Grenoble 1, Institute of Earth Sciences (ISTerre), OSUG/INSU, BP 53, 38041 Grenoble Cedex 9, France

[‡]CNRS and University Joseph Fourier-Grenoble 1, IPAG, OSUG/INSU, BP 53, 38041 Grenoble Cedex 9, France

[§]Physics of Geological Processes, University of Oslo, Norway

[∥]Université de Lyon, Université Lyon 1, Laboratoire des Multimatériaux et Interfaces UMR CNRS 5615, 43 bd du 11 novembre 1918, 69622 Villeurbanne Cedex, France

Supporting Information

**ABSTRACT:** The present study describes a simple and novel synthesis route for submicrometric acicular goethite (α-FeOOH) using high OH/Fe molar ratio (=5) and moderate temperature (30 and 70 °C). Two different alkaline sources (NaOH and $Ca(OH)_2$) and two iron(III) sources ($FeCl_3 \cdot 6H_2O$ and $Fe(NO_3)_3.9H_2O$) were investigated. FESEM, XRD, FTIR, $N_2$ sorption isotherms, color evolution, and pH monitoring have been used to determine the formation mechanism, the particle size, specific surface area, and morphology of goethite particles. Three pH regions were determined during goethite formation, and each of them was qualitatively associated to (I) the formation of a ferric hydroxide gel, leading to acid conditions (pH < 2.5); (II) the spontaneous nucleation of goethite, leading to alkaline conditions (pH > 11) and fine sedimentable particles; and (III) the growth of goethite in alkaline conditions (11 < pH < 13.5). Both the temperature and the Fe(III) source have a significant effect on the particle size, specific surface area, and morphology of goethite. High acicular goethite particles (<1 μm in length, moderate specific surface area, $S_{BET}$ = 31.2 $m^2/g$) were produced after 7 h of reaction at 70 °C, while about 24 h of reaction are required to produce low acicular goethite particles (<0.5 μm in length, high specific surface area, $S_{BET}$ = 133.8 $m^2/g$) at 30 °C, using in both cases iron chloride. When $Ca(OH)_2$ particles are used as alkaline source, a complex mineral composite with high specific surface area (87.3 $m^2/g$) was synthesized; it was mainly composed of unreacted $Ca(OH)_2$ coated with nanosized particles (possibly amorphous iron hydroxide), calcium iron oxide chloride hydrate, and calcite. Novel conditions to prepare uniform goethite particles, possibly with high potential as adsorbents or pigments, have been established.

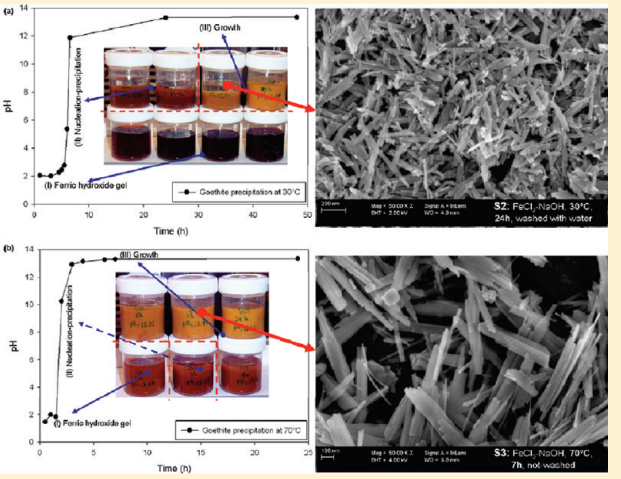


## 1. INTRODUCTION

Iron oxides, hydroxides, and oxy-hydroxides represent efficient sorbents for organic and inorganic species and have a great potential in industrial applications. They are also of substantial interest in environmental sciences, since some of them are frequently occurring in soils and have significant impact on the fate of pollutants.[1] Among iron oxy-hydroxides, goethite (α-FeOOH) is an abundant constituent of terrestrial soils, sediments, and oolitic iron ores and a major weathering product of ferrous silicates (via oxidation and hydrolysis processes). It is predominant in younger sedimentary deposits, giving them a yellowish color.[2−5] Goethite particles have high specific surface areas and strong affinities for oxyanions and heavy metals.[6,7] Recently, the mineral goethite has also been suspected as a constituent of the Martian dusts and dark asteroids.[8]

The mineral goethite has a long history of applications, since it was used as a dark-yellow ochre pigment in paleolithic cave painting over 30 000 years ago. As a colloidal system, it readily forms crystallites of colloidal dimensions, which can be stabilized in water at pH below about 4.[9] It is also a model adsorbent in soils and environmental applications (see ref 10 and references therein). Moreover, goethite finds application as a precursor in magnetic carrier systems, where it can be transformed by thermal treatment into maghemite ($\gamma$-$Fe_2O_3$) or into metallic particles.[6,11]

The synthesis of goethite has been studied for decades (e.g., refs 12−20), and studies to improve the existing methods

**Received:** December 18, 2010
**Revised:** April 13, 2011
**Published:** April 25, 2011

**Table 1. Summary of Synthesis Routes and Main Physicochemical Conditions for Goethite**

| | | precursor | | | synthesis of goethite[a] | | | | |
|---|---|---|---|---|---|---|---|---|---|
| Fe source | additive | method | $T$ (°C) | OH/Fe | $T$ (°C) | pH | $T$ (day) | OH/Fe | ref |
| Fe(III) | not used | fast-mixture of solutions (Fe and MOH) | 20−25 | 0.5−2.5 | 4−90 | constant between 3 and 13 | 6−68 | <2.5 | 12, 14, 18, 26 |
| Fe(III) | not used | titration until pH = 4−12 | 20−25 | nr | 25−80 | constant between 4 and 12 | 7−9 or until 23 years | <2.5 | 3, 9, 15, 18, 21, 25 |
| Fe(III) | yes | titration until pH = 4−12 | 20−25 | nr | 30−90 | constant between 2 and 13 | <6 h | <2.5 | 23, 24, 28 |
| Fe(III) | not used | not necessary | | | 30 | variable during reaction (see Figure 1) | 24 h | 5 | this study |
| Fe(III) | not used | not necessary | | | 70 | variable during reaction (see Figure 1) | 7 h | 5 | this study |
| Fe(0) and Fe (II) | The reaction mechanisms and kinetics for goethite synthesis using Fe(0) and Fe(II) are controlled by iron oxidation. This limits the comparison with the above methods. For specific details, refer to refs 11, 16, 17, 19, 20, and 27). | | | | | | | | |

[a] Implying batch system, dialysis (semicontinuous reactor), or continuous flow microreactors. Fe(III): mainly $Fe(NO_3)_3 \cdot 9H_2O$ or $FeCl_3 \cdot 6H_2O$. Alkaline source (OH): mainly NaOH or KOH. Additive: e.g. hydrazine sulfate, oleic acid, and xylene.

and/or to develop innovative routes to obtain various shapes and sizes of nanosized-to-submicrometric goethite particles continue (e.g., refs 21−26). Generally, the efforts for goethite synthesis are aimed at using Fe(III) solutions or Fe(II) solutions in the presence of an oxidant. More recently, the use of surfactants and other organic compounds for goethite synthesis had also been performed in order to control size and shape (e.g., refs 27 and 28). Table 1 summarizes the main synthesis methods carried out at the laboratory scale that are using exclusively ferric salts as iron source. The methods using Fe(0) and Fe(II) were excluded because the formation of goethite in both cases is strongly controlled by the oxidation of iron, limiting the comparison with studies that use Fe(III) for the iron source. As reported in Table 1, the synthesis of mineral goethite using Fe(III) is classically started by the precipitation of a precursor (ferrihydrite and/or amorphous iron hydroxide) from homogeneous solution. Then, upon aging, the precursor is consumed and goethite particles grow within a few days, with the reaction time mainly depending on the temperature and pH. However, a simple and facile test in the laboratory shows that acicular goethite particles can be instantaneously synthesized at room temperature by adding directly Fe(III) salt or Fe(III) solution in a concentrated NaOH solution (1 M) (see Figure SI-A). This simple test shows that the ferrihydrite and/or amorphous iron hydroxide are not unique precursors for goethite synthesis. Based on this observation, we propose in the present study a simple and novel synthesis route for submicrometric acicular goethite (α-FeOOH) using high initial OH/Fe molar ratio (=5) and moderate temperature (30 and 70 °C). Under these conditions, the Fe(III) is rapidly hydrolyzed, forming a ferric hydroxide gel; this leads to acidic conditions (pH < 2.5) during the first hours of reaction. Subsequently, the nucleation and growth processes of acicular goethite from ferric hydroxide gel produce a drastic pH change in the system, leading to alkaline conditions (13 < pH < 13.5). Two different alkaline sources (NaOH and $Ca(OH)_2$) and two iron(III) sources ($FeCl_3 \cdot 6H_2O$ and $Fe(NO_3)_3 \cdot 9H_2O$) were investigated. FESEM, XRD, FTIR, $N_2$ sorption isotherms, color evolution, and pH monitoring were used to determine the formation mechanism, the particle size, the specific surface area, and the morphology of goethite particles.

## 2. MATERIALS AND METHODS

**2.1. Synthesis of Goethite (Stirred Reactor).** One liter of high-purity water with electrical resistivity of 18.2 MΩ·cm, 1 mol of alkaline source (NaOH or $Ca(OH)_2$), and 0.2 mol of Fe(III) source ($FeCl_3 \cdot 6H_2O$ or $Fe(NO_3)_3 \cdot 9H_2O$) were placed in a titanium reactor (autoclave with internal volume of 2 L). This aqueous reactive system was immediately stirred using constant mechanical agitation (400 rpm) during the reaction. The aqueous system was then heated at 30 or 70 °C for 7 or 24 h by using a heating jacket adapted to the reactor. One additional experiment ($H_2O$−NaOH−$FeCl_3$) was carried out at 30 °C for 10 days in order to evaluate the effect of longer reaction time. The experimental conditions for all syntheses are summarized in Table 1.

At the end of the experiment, the autoclave was removed from the heating system and immersed in cold water when the experiment was carried out at 70 °C. After water cooling at 30 °C (about 10 min), the autoclave was disassembled, and the solid product was carefully recovered and separated by centrifugation (30 min at 12 000 rpm) and decanting the supernatant solutions. The solid product from syntheses of S1 and S2 (see Table 1) was washed two times by redispersion/centrifugation processes in order to remove the halite (NaCl) coprecipitated during the synthesis. Finally, the solid product was dried directly in the centrifugation flasks at 60 °C for 48 h. The dry solid product was manually recovered, weighed, and stored in plastic flasks for further characterizations (FESEM, XRD, and FTIR).

Additionally, a semibatch system (sampling with time) was performed in order to monitor the pH (using MA235 pH/ion analyzer) and follow the color evolution of the colloidal dispersion (from ferric hydroxide gel to goethite dispersion). In this case, about 25 mL of dispersion were sampled in the reactor as a function of time (0.16, 0.5, 1, 3, 4, 6, 7, and 24 h) at 30 °C and (0.5, 1, 2, 3, 4, 6, 7, 24 h) at 70 °C during nucleation and growth of goethite. In these two experiments, the alkaline source and the Fe(III) source were NaOH and $FeCl_3 \cdot 6H_2O$, respectively.

**2.2. FESEM Observations.** The powder samples were dispersed by ultrasonic treatment in absolute ethanol for 5−10 min. One or two drops of suspension were then deposited directly on an aluminum support for SEM observations and coated with platinum. Morphological observations of various selected powders were performed using a Zeiss Ultra 55 field emission gun scanning electron microscope (FESEM) that has a maximum spatial resolution of approximately 1 nm at 15 kV.

**2.3. FTIR Measurements.** The powder samples were also characterized by using infrared spectrometry, with a BRUKER HYPERION

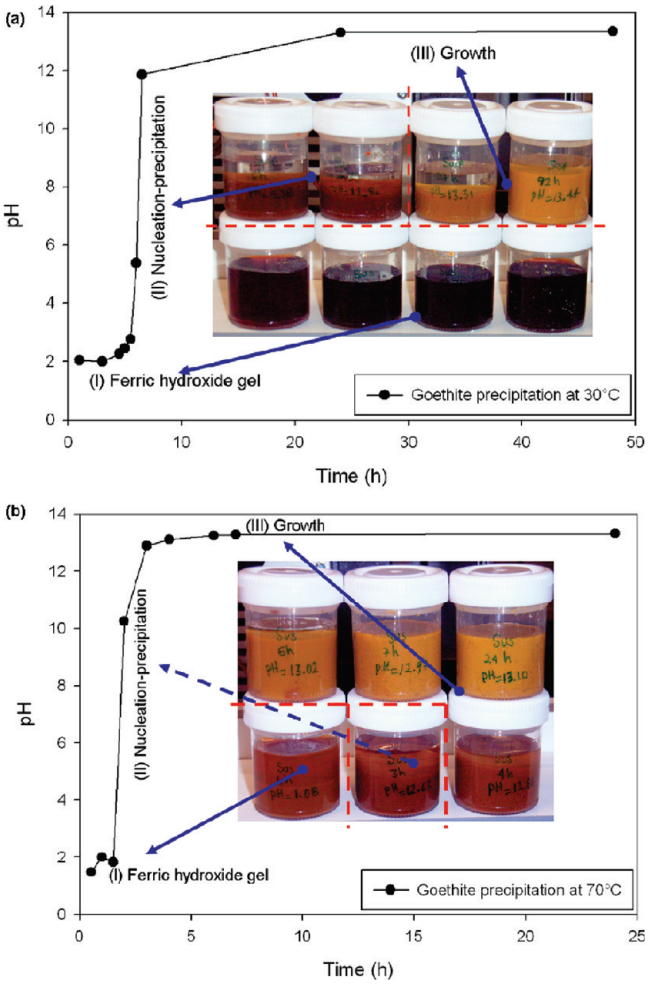


**Figure 1.** Kinetic behavior of pH and color of colloidal dispersion during formation of acicular goethite at 30 °C (a) and 70 °C (b).

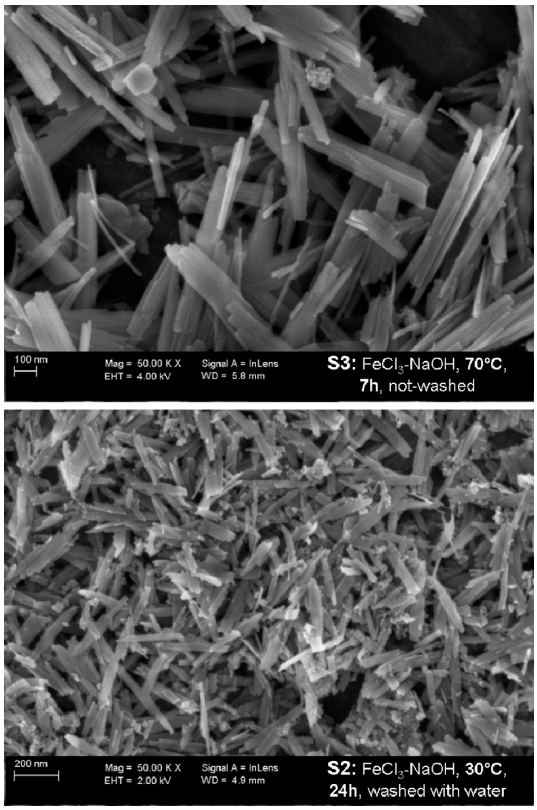


**Figure 2.** Well crystallized acicular goethite particles precipitated from ferric hydroxide gel at 70 °C (after 7 h of reaction) and at 30 °C (after 24 h of reaction). For both cases, $FeCl_3 \cdot 6H_2O$ and NaOH were used as Fe(III) and ($OH^-$), respectively.

3000 infrared microscope in transmission mode, with a MCT mono-detector at 4 $cm^{-1}$ resolution. The typical size of the infrared spot on the sample was ~50 × 50 $\mu m^2$. For these measurements, some fine aggregates of solid products were manually compressed between two KBr windows in order to deposit a thin film of sample on a KBr window.

**2.4. XRD Measurements.** X-ray powder diffraction (XRD) analyses were performed using a D5000, SIEMENS diffractometer in Bragg−Brentano geometry, equipped with a goniometer theta−theta with a rotating sample holder. The XRD patterns were collected using Cu K$\alpha_1$ ($\lambda_{K\alpha1}$ = 1.5406 Å) and K$\alpha_2$ ($\lambda_{K\alpha2}$ = 1.5444 Å) radiation in the range $2\theta$ = 10−70° with a step size of 0.04° and a counting time of 6 s per step.

**2.5. $N_2$ Sorption Isotherms.** Three $N_2$ sorption isotherms for the S1, S2, and S6 samples were performed by using a sorptomatic system (Thermo Electron Corporation). The specific surface area of powdered S1, S2, and S6 samples was estimated by applying the Brunauer−Emmet−Teller (BET) equation in the $0.05 \leq P/P_0 \leq 0.35$ interval of relative pressure and by using 16.2 $Å^2$ for the cross-sectional area of molecular $N_2$. A nonlinear regression by the least-squares method was performed to fit the interval data ($n_{ads}$ *vs* $P/P_0$) in the experimental isotherms.

## 3. RESULTS AND DISCUSSION

**3.1. Mechanism of Goethite Formation.** It has been proposed that the ferrihydrite and/or amorphous iron hydroxide are crucial precursors for goethite synthesis (see Table 1). The precursor−goethite transformation, via dissolution of the precursor nanoparticles followed by precipitation to oriented aggregation accompanied by phase transformation,[26] takes several hours or days under acidic conditions (pH < 3) or alkaline conditions (pH > 12), depending on the reaction temperature. However, we tested that acicular goethite particles can be instantaneously synthesized at room temperature (19 °C) by adding directly Fe(III) salt or Fe(III) solution in a concentrated NaOH solution (1 M) (see Figure SI-A). This indicates that the ferrihydrite and/or amorphous iron hydroxide are not exclusive precursors for goethite synthesis.

In our experiments, we demonstrate that this precursor is not necessary to produce submicrometric acicular goethite (α-FeOOH) using high initial OH/Fe molar ratio (=5) and moderate temperature (30 and 70 °C). Goethite formation is characterized by the presence of three successive pH domains; they are specifically associated with (I) the formation of ferric hydroxide gel (FeHgel), leading to acid conditions (pH < 2.5); (II) the spontaneous nucleation of goethite from FeHgel, leading to alkaline conditions (pH > 11) and the first sedimentable particles; and (III) the growth of goethite in alkaline conditions (11 < pH < 13.5). These three steps or pH domains during goethite formation are well correlated with color evolution (see Figure 1). The kinetic behavior (pH-color evolution) depends on the reaction temperature; globally the nucleation−growth of goethite at 70 °C was close to three times faster than that at 30 °C. The results reveal that well-crystallized goethite particles


dx.doi.org/10.1021/cg1016802 |*Cryst. Growth Des.* 2011, 11, 2264–2272

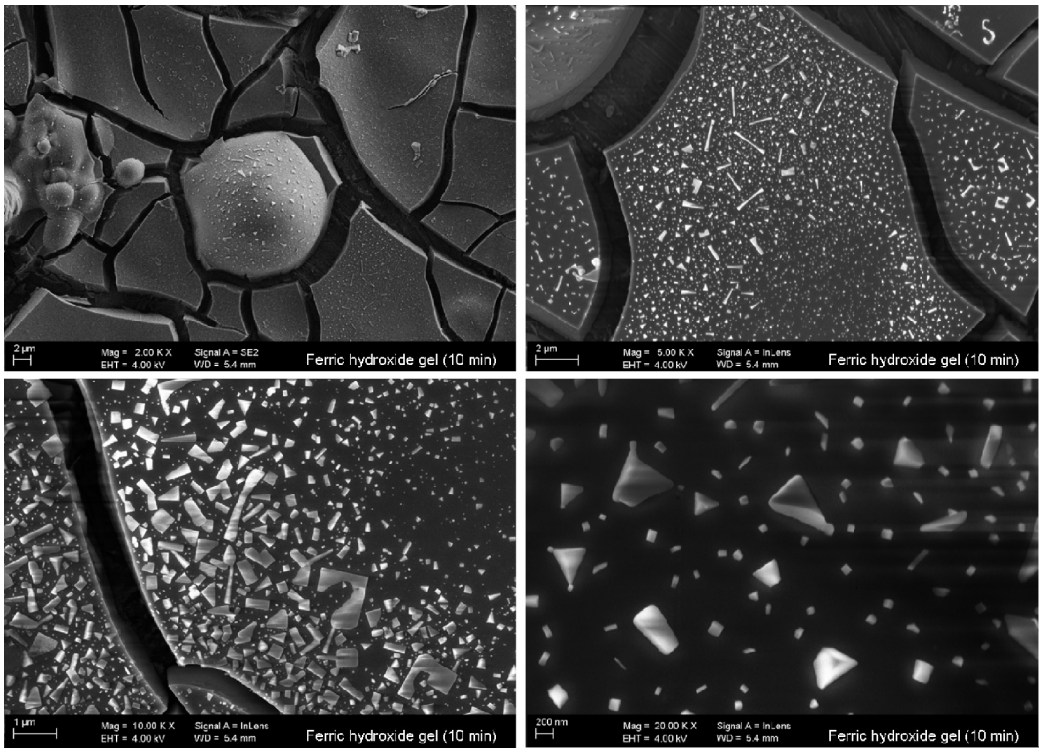


**Figure 3.** FESEM images showing the microscopic aspect of the ferric hydroxide gel after 10 min of reaction at 30 °C.

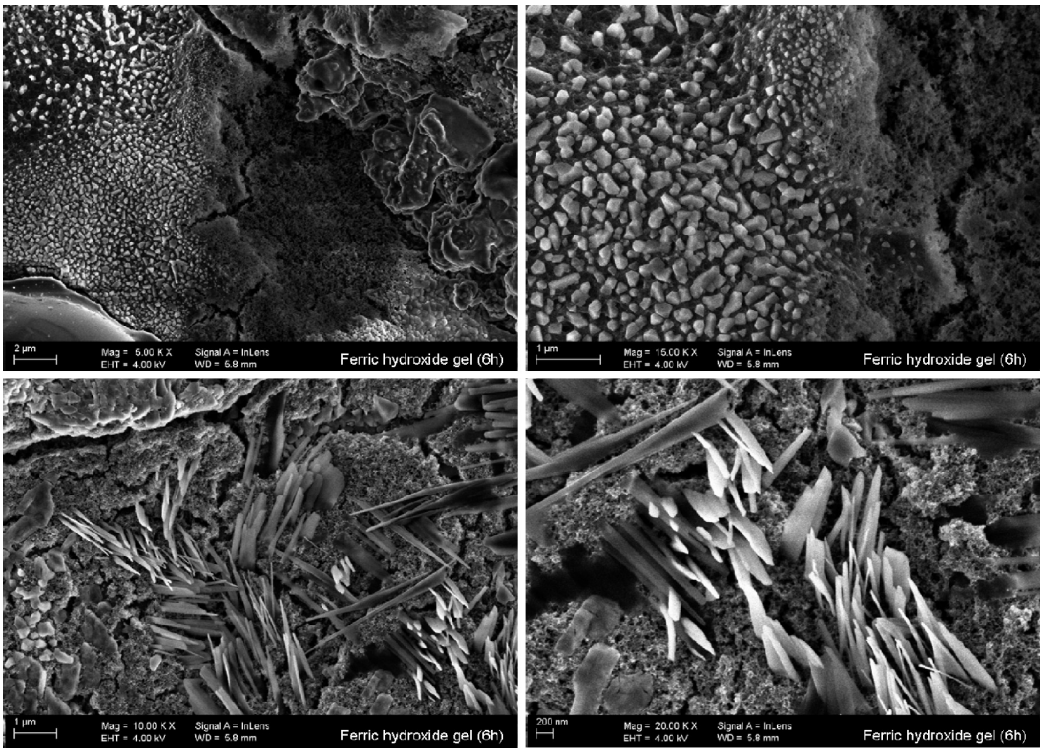


**Figure 4.** FESEM images showing the first goethite particles precipitated from the ferric hydroxide gel after 6 h of reaction at 30 °C.

(high acicular goethite <1 $\mu$m in length) are produced after 7 h of reaction at 70 °C. Conversely, about 24 h of reaction are required to produce well-crystallized goethite particles (low acicular goethite <0.5 $\mu$m in length) at 30 °C using, in both cases, the same Fe(III) and ($OH^-$) sources, i.e. $FeCl_3 \cdot 6H_2O$ and NaOH, respectively (see Figure 2).

*3.1.1. Formation of Ferric Hydroxide Gel.* The notion of ferric gels was introduced in the early 20th century (e.g., ref 29). In the


dx.doi.org/10.1021/cg1016802 |*Cryst. Growth Des.* 2011, 11, 2264–2272

early 1990s, sophisticated structural measurements (X-ray absorption spectroscopy) were performed by Combes et al.[30,31] to investigate the atomic organization at boundaries of Fe(III) during formation of various oxy-hydroxides. In those studies, the degree of structural order, atomic shells, coherent domain sizes, etc. in powdered samples were reported. In our study, we used electron microscopy (FESEM) and optical observations (color evolution reported in Figure 1) to elucidate only the physical aspect and semiquantitative composition of so-called ferric hydroxide gel. This has not been reported to the best of our knowledge. The FESEM images in Figure 3 show the FeHgel aspect after 10 min of reaction. Herein, microscopic cracks were generated during gel drying and observed on FESEM images. Microscopic particles on the surface of the dried gel were also observed, but they were possibly formed during the drying process, because these particles are very fragile to the electron beam; that is, the particles are rapidly transformed/dehydrated during FESEM measurements. The main elemental composition for FeHgel is Fe, O, and Na, measured by using semiquantitative EDS analyses. This indicates that the excess of NaOH in the system plays a significant role in the formation of the FeHgel. The acidic pH in a colloidal dispersion during this reaction step (see Figure 1) is in agreement with this assumption. In situ measurements, by coupling a reaction system with Raman/infrared spectroscopy would be required to obtain more specific insights on the composition, formation mechanism, and kinetic behavior of this FeHgel.

*3.1.2. Nucleation of Goethite from Ferric Hydroxide Gel.* The color and pH of FeHgel changed slightly with time before the nucleation process of goethite, as observed in the synthesis at 30 °C (Figure 1a). Conversely, the viscosity of FeHgel seems to have increased with time (similar to a polymerization process) until goethite nucleation. When the nucleation process of goethite took place from the FeHgel (after about 6 h of reaction at 30 °C), the pH increased drastically, leading to highly alkaline conditions (see Figure 1a), due to $OH^-$ liberation from the transformation of the FeHgel into the first goethite particles (see Figure 4). This pH increase was also associated with a color

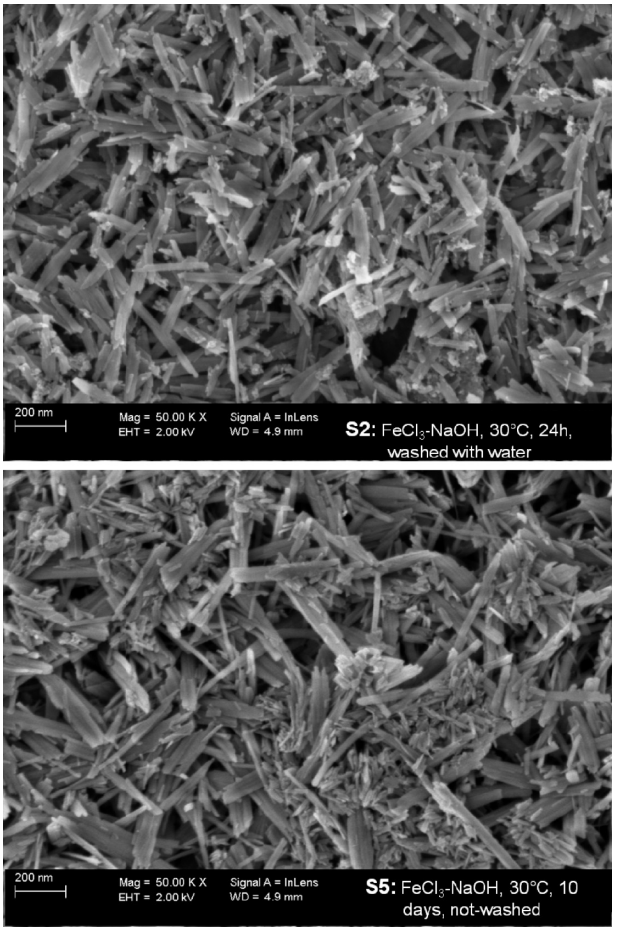


**Figure 5.** FESEM images showing a slight Ostwald coarsening process from 1 to 10 days for goethite growth at 30 °C.

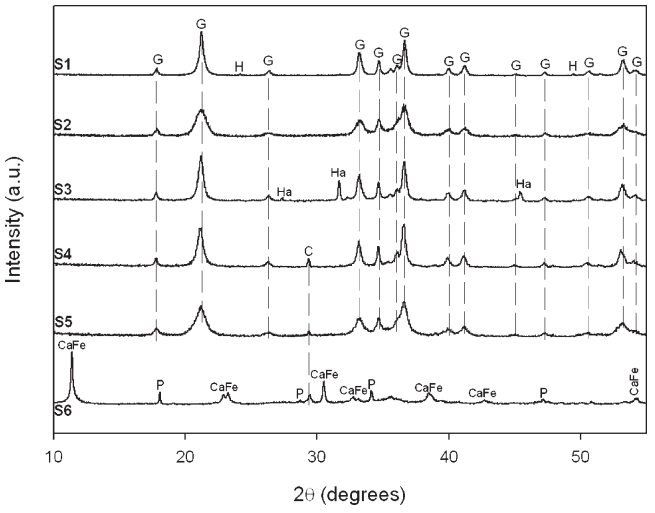


**Figure 6.** X-ray diffraction (XRD) patterns of six different syntheses (see experimental conditions in Table 1): G, goethite; H, hematite; Ha, halite; C, calcite; CaFe, calcium iron oxide chloride hydrate; P, portlandite.

**Table 2. Experimental Conditions for Goethite Synthesis and Mineral Composition of Solid Products Determined by XRD**

| synthesis | OH/Fe[a] | $T$ (°C) | Fe(III) | OH | washing | time | product (s) |
|---|---|---|---|---|---|---|---|
| S1 | 5 | 70 | $FeCl_3 \cdot 6H_2O$ | NaOH | yes | 24 h | G, H[b] |
| S2 | 5 | 30 | $FeCl_3 \cdot 6H_2O$ | NaOH | yes | 24 h | G |
| S3 | 5 | 70 | $FeCl_3 \cdot 6H_2O$ | NaOH | not | 7 h | G, Ha[b] |
| S4 | 5 | 70 | $Fe(NO_3)_3 \cdot 9H_2O$ | NaOH | not | 7 h | G, C[b] |
| S5 | 5 | 30 | $FeCl_3 \cdot 6H_2O$ | NaOH | not | 10 days | G, C[b] |
| S6 | 5 | 70 | $FeCl_3 \cdot 6H_2O$ | $Ca(OH)_2$ | not | 24 h | CaFe, P, C[b] |

[a] OH/Fe molar ratio. [b] Slight proportion; G, goethite (α-FeOOH); H, hematite ($\alpha$-$Fe_2O_3$); Ha, halite (NaCl); C, calcite ($CaCO_3$); CaFe, calcium iron oxide chloride hydrate ($Ca_2FeO_3Cl \cdot 5H_2O$); P, portlandite ($Ca(OH)_2$).


dx.doi.org/10.1021/cg1016802 |*Cryst. Growth Des.* 2011, 11, 2264–2272

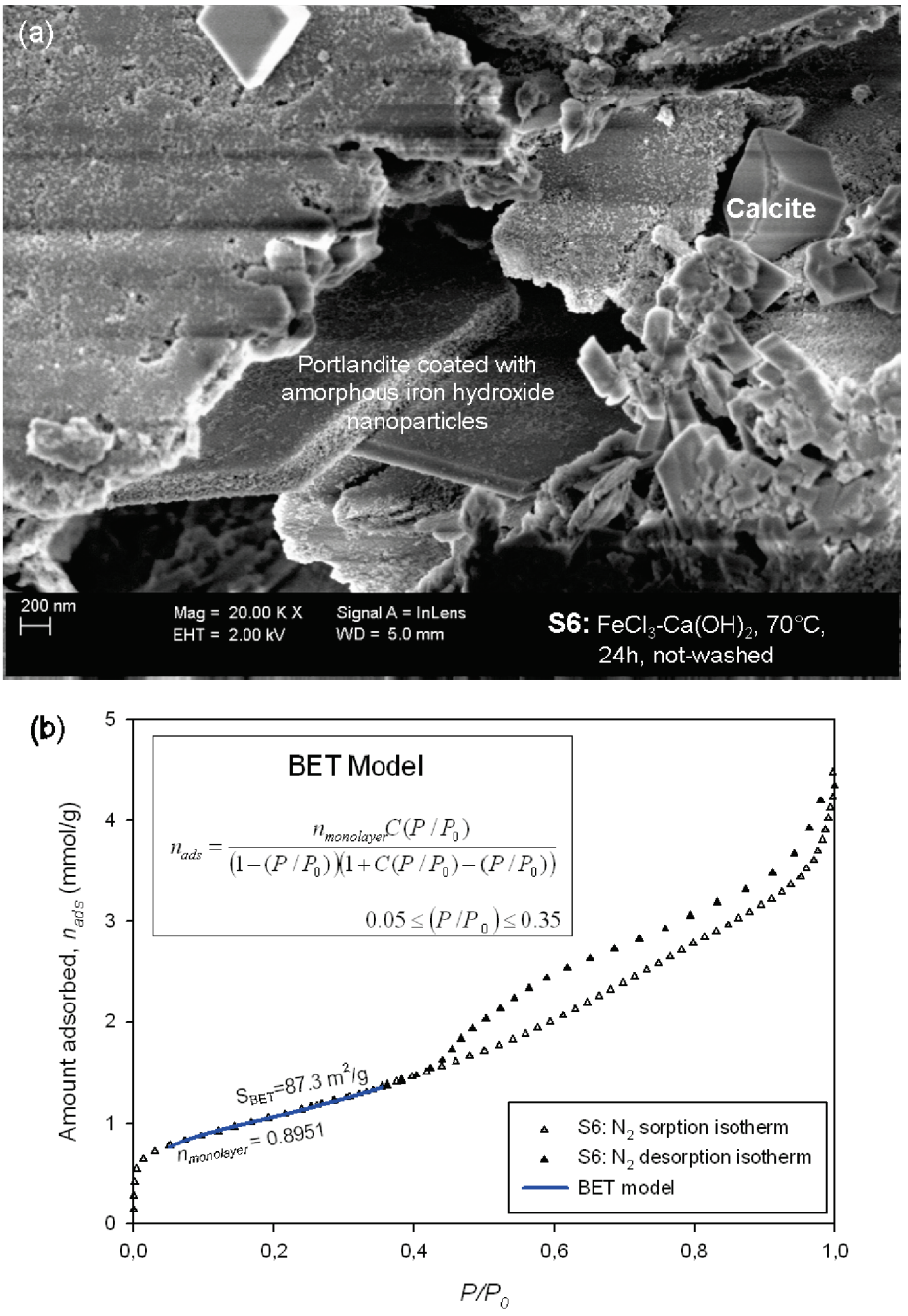


**Figure 7.** (a) FESEM micrograph showing a complex mineral composite (S6) containing calcium iron oxide chloride hydrate, portlandite, calcite (see also Figure 6), and possibly amorphous iron hydroxide nanoparticles. (b) $N_2$ experimental sorption−desorption isotherms for the S6 sample and the BET model fitting the experimental data between 0.05 and 0.35 of relative pressure.

change of the dispersion from dark brown to orange-brown as shown in Figure 1.

*3.1.3. Growth of Goethite.* In our experiments, the growth process of acicular goethite particles takes place under alkaline conditions (11 < pH < 13.5). The pH equilibration after several hours of reaction indicates a macroscopic equilibrium between goethite and the interacting alkaline solution (see Figure 1). As mentioned previously, high amounts of acicular goethite (<1 $\mu$m in length) were grown after 7 h of reaction at 70 °C, while about 24 h of reaction are required to produce well-crystallized goethite particles (low acicular goethite <0.5 $\mu$m in length) at 30 °C (see Figure 2). Additionally, for goethite formation at 30 °C, a moderate Ostwald coarsening process was observed from one day to 10 days (see Figure 5), and the average particle size (in length) increased from 250 ± 35 to 395 ± 50 nm.

**3.2. Mineral Composition.** Under the conditions of our study (Table 2), single-phase goethite particles are formed for OH/Fe molar ratio (=5), as determined by X-ray diffraction (Figure 6). Small proportions of calcite, hematite, and halite were also identified in specific samples. When $Ca(OH)_2$ particles are used as alkaline source (synthesis S6), a complex mineral composite


dx.doi.org/10.1021/cg1016802 |*Cryst. Growth Des.* 2011, 11, 2264–2272

was synthesized. This powdered material was mainly composed of unreacted $Ca(OH)_2$ coated by nanosized particles (possibly amorphous iron hydroxide) (see Figure 7a), well crystallized particles characterized as calcium iron oxide chloride hydrate ($Ca_2FeO_3Cl\cdot 5H_2O$) from XRD pattern (ICDD # 044-0445) (see Figure 6), and calcite (minor proportion). The specific surface area ($S_{BET}$ = 87.3 $m^2/g$) has been measured using a $N_2$ sorption isotherm (see Figure 7b). We note that the XRD results are in agreement with FTIR measurements (Figure 8). For example, the deformational modes of hydroxyls (out-of-plane around 780−800 $cm^{-1}$ and in-plane around 880−900 $cm^{-1}$) typical for goethite are well-defined in the syntheses of S1-to-S5. Conversely, these deformational modes of hydroxyls are absent in the synthesis of S6, indicating the absence of the goethite phase. In this latter case, a complex hydration state of the solid was observed in the stretching region for OH and $H_2O$. Based on XRD results, we assumed the presence of adsorbed water, structural molecular water, and structural −OH groups in the solid product. The −OH stretching vibration bands for portlandite are well-defined[32] but poorly characterized for amorphous iron hydroxide suspected in S6 (see also Figure 7a).

**3.3. Morphology and Size.** The morphology and average size of goethite particles were deduced from FESEM observations; the length and width of particles were manually measured on 50 isolated particles for five syntheses (S1-to-S5), and the average values are summarized in Table 3. Based on these results, the goethite was classed as low, moderate, and high acicular goethite. Concerning the particle size, two important points are here mentioned. First, the particle size (in length) increases with an increase of temperature (see Figure 2), as early reported in the literature (e.g., ref 14). Second, the length and width of goethite particles depend on the Fe(III) source: when ferric nitrate is used, smaller particles (in length) of goethite are synthesized compared with those for the ferric chloride source at the same temperature of reaction (see S3 image in Figure 2 and S4 image in Figure 9). This could be due to adsorption and/or incorporation of nitrate oxyanions during nucleation−growth of goethite crystals. Several studies have demonstrated that the crystal growth processes are often influenced by the presence of foreign ions, molecules, and/or additives, leading to significant changes in the morphology, average particle size, particle size distribution, specific surface area, etc. (e.g., refs 33 and 34). Finally, we note that the FESEM observations/measurements on the particle size are in agreement with specific surface areas determined from $N_2$ sorption isotherms for syntheses S1 and S2 (see Table 3 and Figure 10). Typically, the specific surface area increases with a decrease of particle size. In our study, the goethite synthesized at 30 °C (S2) has a high specific surface area ($S_{BET}$ = 133.8 $m^2/g$). Conversely, a moderate specific surface area ($S_{BET}$ = 31 $m^2/g$) was determined for goethite synthesized at 70 °C (S1), as illustrated directly in the $N_2$ sorption isotherms (Figure 10). A submicrometric size of particles and high specific surface area suggest a high potential as adsorbent for goethite synthesized at 30 °C.

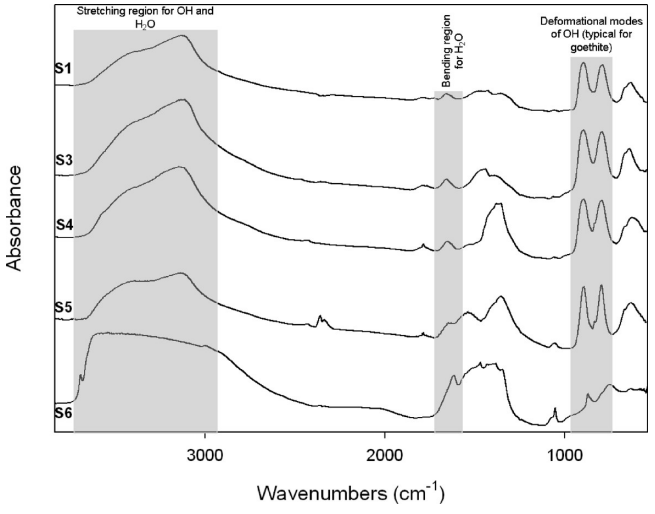


**Figure 8.** FTIR measurements underlining vibration modes for goethite in stretching and bending regions and also underlining the deformational modes of hydroxyls typically observed for the goethite-phase.

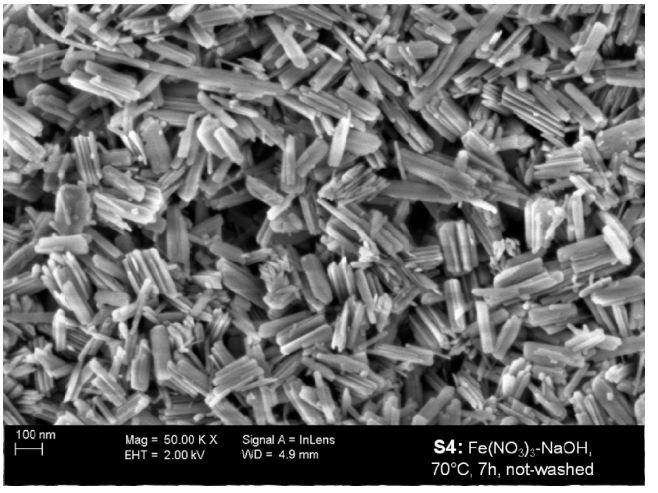


**Figure 9.** FESEM micrograph showing low acicular goethite (S4) synthesized from the water−$Fe(NO_3)_3$−NaOH system at 70 °C.

**Table 3. Morphology and Average Size of Goethite Particles Measured from FESEM Observations**[a]

| | | FESEM | | | $N_2$ sorption isotherms |
|---|---|---|---|---|---|
| synthesis | morphology | L: length (nm) | W: width (nm) | L/W ratio | $S_{BET}$ ($m^2/g$) |
| S1 | high acicular | 750 ± 100 | 60 ± 20 | 12.5 | 31.2 |
| S2 | low acicular | 250 ± 35 | 65 ± 20 | 3.8 | 133.8 |
| S3 | moderate acicular | 610 ± 40 | 85 ± 30 | 7.17 | |
| S4 | low acicular | 190 ± 10 | 70 ± 15 | 2.7 | |
| S5 | low acicular | 395 ± 50 | 80 ± 20 | 4.8 | |

[a] Specific surface areas ($S_{BET}$) for syntheses S1 and S2 determined from $N_2$ sorption isotherms (Figure 10).


dx.doi.org/10.1021/cg1016802 |Cryst. Growth Des. 2011, 11, 2264–2272

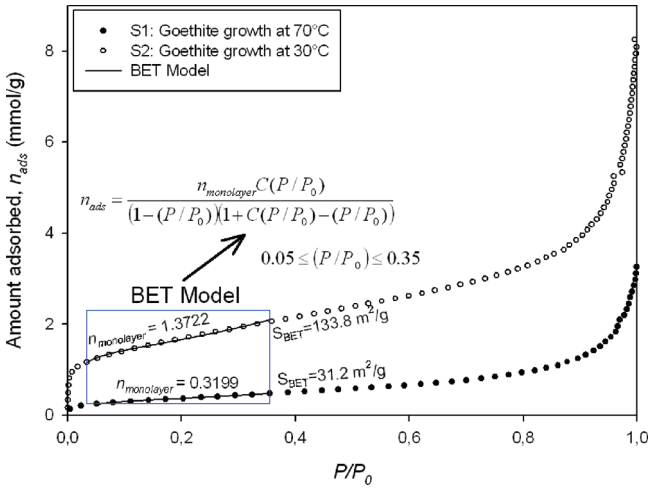


**Figure 10.** $N_2$ experimental sorption isotherms for S1 and S2 samples and the BET model fitting the experimental data between 0.05 and 0.35 of relative pressure.

## 4. CONCLUSION

The main aim for this study is to propose a simple and novel synthesis route for submicrometric acicular goethite (α-FeOOH) using high OH/Fe molar ratio (=5) and moderate temperature (30 and 70 °C). FESEM, XRD, FTIR, $N_2$ sorption isotherms, color evolution, and pH monitoring were used to provide precious insights on the formation mechanism, particle size, specific surface area, and morphology of goethite. Three pH regions or domains characterize the process of goethite formation:

(I) the formation of a ferric hydroxide gel, leading to acid conditions (pH < 2.5),

(II) the spontaneous nucleation of goethite, leading to alkaline conditions (pH > 11) and fine sedimentable particles, and

(III) the growth of goethite in alkaline conditions (11 < pH < 13.5).

Macroscopic ex-situ measurements (pH and color evolution) show a complex kinetic behavior of the ferric hydroxide gel before nucleation of goethite. In situ measurements, i.e. coupling a reaction system with Raman/infrared spectroscopy (immersed sensors) often used in the fabrication of pharmaceutical compounds, would be required to obtain more specific insights on the composition and kinetic behavior of such gel.

High acicular goethite (<1 μm in length) with moderate specific surface area (31.2 $m^2/g$) was produced at 70 °C. Conversely, low acicular goethite (<0.5 μm in length) with high specific surface area (133.8 $m^2/g$) was produced at 30 °C. In both cases, iron chloride was the Fe(III) source. Submicrometric size of particles, morphology, high purity, and high specific surface area (mainly for synthesis at 30 °C) suggest a high potential as adsorbent.

## AUTHOR INFORMATION

### Corresponding Author

*E-mail address: german.montes-hernandez@obs.ujf-grenoble.fr.

## ACKNOWLEDGMENT

The authors are grateful to the National Research Council (CNRS), France, for providing financial support for this work.

## ASSOCIATED CONTENT

**Supporting Information.** Figure SI-A: Diagram of reaction to produce goethite at room temperature, and FESEM image showing the instantaneous precipitation of irregular submicrometric particles of acicular goethite at room temperature. This material is available free of charge via the Internet at http://pubs.acs.org.

## REFERENCES

(1) Aquino, A. J. A.; Tunega, D.; Haberhauer, G.; Gerzabek, M. H.; Lischka, H. *Geochem. Cosmochem. Acta* **2008**, *72*, 3587.

(2) Nayak, R.; Rao, J. R. *J. Sci. Ind. Res.* **2005**, *64*, 35.

(3) Prasad, P. S. R.; Prasad, K. S.; Chaintanya, V. K.; Babu, E. V. S. S. K.; Sreedhar, B.; Murthy, S. R. *J. Asian Earth Sci.* **2006**, *27*, 503.

(4) Cornell, R. M.; Schwertmann, U. *The Iron Oxides*; VCH: Weinheim, Germany, 1996.

(5) Ozdemir, O.; Dunlop, D. J. *Earth Planet. Sci. Lett.* **2000**, *177*, 59.

(6) Schwertmann, U.; Cornell, R. M. *Iron oxides in the laboratory: Preparation and Characterization*; VCH: Weinheim, Germany, 1991.

(7) Hayes, K. F.; Roe, A. L.; Brown, G. E., Jr.; Hodgson, K. O.; Leckie, J. O.; Parks, G. A. *Science* **1987**, *238*, 783.

(8) Beck, P. ; Quirico, E.; Sevestre, D.; Montes-Hernandez, G.; Pommerol, A.; Schmitt, B. *Astronomy & Astrophysics* **2010**, DOI: 10.1051/0004-6361/201015851

(9) Thies-Weesie, D. M. E.; Hoog, J. P.; Hernandez Mendiola, M. H.; Petukhov, A. V.; Vroege, G. J. *Chem. Mater.* **2007**, *19*, 5538.

(10) Kosmulski, M.; Durand-Vidal, S.; Maczka, E.; Rosenhold, J. B. *J. Colloid Interface Sci.* **2004**, *271*, 261.

(11) Núñez, N. O.; Tartaj, P.; Puerto Morales, M.; Pozas, R.; Ocaña, M.; Serna, C. J. *Chem. Mater.* **2003**, *15*, 3558.

(12) Van Der Woude, J. H. A.; De Bruyn, P. L. *Colloids Surf.* **1984**, *12*, 179.

(13) Ford, R. G.; Bertsch, P. M.; Seaman, J. C. *Clays Clay Miner.* **1997**, *45*, 769.

(14) Schwertmann, U.; Cambier, P.; Murad, E. *Clays Clay Miner.* **1985**, *33*, 369.

(15) Christensen, A. N.; Jensen, T. R.; Bahl, C. R. H.; DiMasi, E. *J. Solid Sate Chem.* **2007**, *180*, 1431.

(16) Gilbert, F.; Refait, P.; Lévêque, F.; Ramazeilles, C.; Conforto, E. *J. Phys. Chem. Solids* **2008**, *69*, 2124.

(17) Kurokawa, H.; Senna, M. *Mater. Sci. Eng. B* **2006**, *135*, 55.

(18) Kosmulski, M.; Maczka, E.; Jartych, E.; Rosenholm, J. B. *Adv. Colloid Interface Sci.* **2003**, *103*, 57.

(19) Siles-Dotor, M. G.; Bokhimi; Morales, A.; Benaissa, M.; Cabral-Prieto, A. *Nanostruct. Mater.* **1997**, *8*, 657.

(20) Cabral-Prieto, A.; Reyes-Felipe, A. A.; Siles-Dotor, M. G. *Nanostruct. Mater.* **1998**, *10*, 311.

(21) Abou-Hassan, A.; Sandre, O.; Neveu, S.; Cabuil, V. *Angew. Chem.* **2009**, *121*, 2378.

(22) Nuñez, N. O.; Puerto Morales, M.; Tartaj, P.; Serna, C. J. *J. Mater. Chem.* **2000**, *10*, 2561.

(23) Mohapatra, M.; Rout, K.; Gupta, S. K.; Singh, P.; Anand, S.; Mishra, B. K. *J. Nanopart. Res.* **2010**, *12*, 681.

(24) Mohapatra, M.; Gupta, S. K.; Satpati, B.; Anand, S.; Mishra, B. K. *Colloids Surf., A: Physicochem. Eng. Aspects* **2010**, *355*, 53.

(25) Bakoyannakis, D. N.; Deliyanni, E. A.; Zouboulis, A. I.; Matis, K. A.; Nalbandian, L.; Kehagias, Th. *Microporous Mesoporous Mater.* **2003**, *59*, 35.

(26) Penn, R. L.; Erbs, J. J.; Gulliver, D. M. *J. Cryst. Growth* **2006**, *293*, 1.

(27) Frost, R.; Zhu, H. Y.; Wu, P.; Bostrom, T. *Mater. Lett.* **2005**, *59*, 2238.

(28) Yu, T.; Park, J.; Moon, J.; An, K.; Piao, Y.; Hyeon, T. *J. Am. Chem. Soc.* **2007**, *129*, 14558.

(29) Perry, J. H. *Ind. Eng. Chem.* **1927**, *19*, 746.

(30) Combes, J. M.; Manceau, A.; Calas, G.; Bottero, J. Y. *Geochem. Cosmochem. Acta* **1989**, *53*, 583.

(31) Combes, J. M.; Manceau, A.; Calas, G. *Geochem. Cosmochem. Acta* **1990**, *54*, 1083.
(32) Montes-Hernandez, G.; Pommerol, A.; Renard, F.; Beck, P.; Quirico, E.; Brissaud, O. *Chem. Eng. J.* **2010**, *161*, 250.
(33) Montes-Hernandez, G.; Fernandez-Martinez, A.; Charlet, L.; Renard, F.; Scheinost, A.; Bueno, M. *Cryst. Growth Des.* **2008**, *8*, 2497.
(34) Montes-Hernandez, G.; Concha-Lozano, N.; Renard, F.; Quirico, E. *J. Hazard. Mater.* **2009**, *166*, 788.